TOXICOLOGICAL SCIENCES **64,** 253–258 (2001)


# *In Vivo* Measurement of Fine and Coarse Aerosol Deposition in the Nasal Airways of Female Long-Evans Rats

James T. Kelly, Carol M. Bobbitt, and Bahman Asgharian[1]

*CIIT Centers for Health Research, 6 Davis Drive, Research Triangle Park, North Carolina 27709*

Received May 1, 2001; accepted August 15, 2001

**Experimental data on fine and coarse aerosol deposition in the nasal airways of animals are essential in appropriately using toxicological studies to assess the potential risk to human health from exposure to airborne pollutants. However, such data are scarce. The objective of this study was to determine aerosol deposition efficiencies for the nasal airways in Long-Evans rats for particles with diameters ranging from 0.5 to 4 $\mu$m. Polystyrene latex (PSL) microspheres in steady-state and pulsatile flows were passed through the nasal airways for simulated inspiratory and expiratory scenarios. Average flow rates ranged from 220 to 640 ml/min. Deposition increased sharply with increasing particle inertia for all exposure scenarios. Expiratory deposition efficiency appeared to be somewhat higher than inspiratory deposition efficiency for both steady-state and pulsatile flow conditions. Pulsatile flow yielded significantly higher deposition than steady-state flow. This result emphasizes the importance of considering fluid accelerations inherent in normal breathing when determining aerosol deposition that is dominated by inertial impaction. Variability in the data, which was suspected to result primarily from the difficult surgical procedure, was in excess of expected intersubject variability. The results of this study will be incorporated into extrapolation-modeling and risk-assessment activities for inhaled pollutants.**

*Key Words:* **Long-Evans rats; deposition efficiency; nasal airway; impaction; *in vivo* deposition.**

Extrapolation models that estimate a delivered dose of inhaled particles to target sites in the human lung are important components in risk assessment for inhaled pollutants (Ménache *et al.*, 1995). These extrapolation models incorporate experimental data on deposition in laboratory animals and provide reasonable estimates of human lung deposition by accounting for inter-species differences. Since rat nasal deposition data have been used extensively in extrapolation models, accurate, thorough experimental data on particle deposition in the nasal airways of the rat are essential.

Deposition of ultrafine particles, or particles with geometric diameters less than 0.1 $\mu$m, in the upper respiratory tracts of rats has been experimentally studied *in vivo* (Chen *et al.*, 1989; Gerde *et al.*, 1991; Wolff *et al.*, 1984) and in nasal molds (Cheng *et al.*, 1990). Deposition of fine and coarse particles, or particles with geometric diameters ranging from about 0.5 to 5 $\mu$m, in rat upper respiratory tracts has been studied *in vivo* (Raabe *et al.*, 1977, 1988) and in nasal molds (Kelly *et al.*, 2001, Schreider, 1983).

The results of studies by Raabe *et al.* (1977, 1988), as discussed in Kelly *et al.* (2001), warrant further research into nasal deposition of fine and coarse particles in the rat. The nasal molds used in the studies by Kelly *et al.* (2001) and by Schreider (1983) were made from postmortem casts of rat nasal airways. The cross-sectional area of a postmortem airway cast has been indicated as being up to twice that of a live subject (Guilmette *et al.*, 1989; Yeh *et al.*, 1997). Tissue shrinkage has been cited as a possible reason for the observed dimensional differences (Guilmette *et al.*, 1989). Differences in morphology between the nasal airways of the live rat and the nasal mold may result in differences in deposition. Therefore, further *in vivo* study of nasal deposition of fine and coarse particles in the rat is warranted.

The objective of this study was to determine aerosol deposition efficiencies, or fractions of particles entering the nose and depositing in the nasal airways of Long-Evans rats, for particles with diameters ranging from 0.5 to 4 $\mu$m.

## MATERIALS AND METHODS

***Animals.*** Twenty-two female Long-Evans rats were obtained from Charles River Breeding Laboratories (Raleigh, NC). The rats were certified to be free of respiratory disease and had a mean ($\pm$ standard deviation) body weight of 327 g ($\pm$ 58 g). Animals were housed 2 per cage in 48 $\times$27 $\times$20 cm polycarbonate cages with Alpha-dri bedding (Shepherd Specialties Paper, Kalamazoo, MI). The temperature in the animal rooms was maintained at 20 $\pm$ 5°C, with a relative humidity of 50 $\pm$ 15%. Animals were kept on a 12-h light cycle (0700–1900). Food (NIH-07 pelleted diet, Zeigler Bros., Gardener's Point, PA) and reverse-osmosis water were provided *ad libitum.*

***Aerosol generation and characterization.*** The experimental apparatus is illustrated in Figure 1A and 1B. Polystyrene latex (PSL) microspheres (density

Although the research described in this manuscript has been funded wholly or in part by the U.S. Environmental Protection Agency's STAR program through grant (R827996-010), it has not been subjected to any EPA review. Therefore the paper does not necessarily reflect the views of the agency, and no official endorsement should be inferred.

[1] To whom correspondence should be addressed. Fax: (919) 558-1213. E-mail: asgharian@ciit.org.

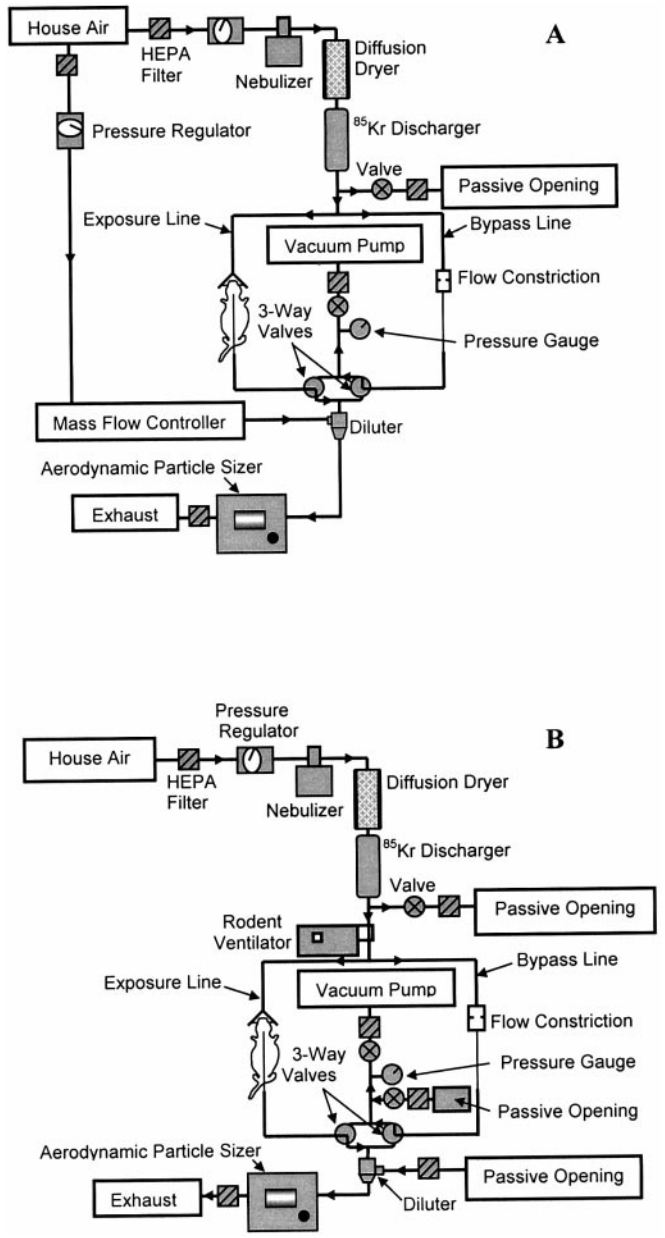


**FIG. 1.** Schematic diagram of the experimental apparatus for (A) steady state and (B) pulsatile flow conditions.

of about 1 g/cm$^3$) were suspended in distilled water and nebulized using a Lovelace nebulizer (In-Tox Products, Albuquerque, NM). PSL microspheres of 10 monodisperse particle diameters ranging from 0.5 to 4.2 $\mu$m (0.5, 0.8, 1.1, 2.1, and 2.8 $\mu$m from Polysciences, Warrington, PA; 1.8, 2.8, 3.2, 3.6, and 4.2 $\mu$m from Spherotech, Inc., Libertyville, IL) were used. Particle sizes were supplied by the manufacturers and verified with an aerodynamic particle sizer (APS) (TSI Model 3320, St. Paul, MN). A dry aerosol with charge Boltzman equilibrium was obtained by passing nebulized droplets through a silica gel diffusion dryer and a 2-mCi $^{85}$Kr neutralizer.

***Exposure.*** A surgical preparation derived from Gerde *et al.* (1991) enabled aerosols to be passed through the animal's nasal airways at steady-state and pulsatile flow rates for simulated inspiratory and expiratory conditions.

Rats were anesthetized prior to exposure with a 0.3-ml intraperitoneal injection of Rompun (xylazine, 20 mg/ml injectable; Bayer Corp., Agriculture Division, Animal Health, Shawnee Mission, KS) in 1:1 combination with Ketaset (ketamine HCL, 100 mg/ml; Fort Dodge Laboratories, Inc., Fort Dodge, IA). Anesthesia was subsequently maintained with small subcutaneous doses (e.g., 0.15 ml) given as required, approximately every 15–30 min, to ensure that the animal remained anesthetized during the entire exposure. A high-intensity lamp was used to maintain the body temperature of anesthetized animals. Animals were killed by exsanguination following exposure.

After anesthetization, the trachea was surgically exposed, and a tracheal incision was made about 2 mm posterior to the larynx and parallel to the tracheal rings. One end of a 14-gauge needle, used as a breathing catheter, was immediately inserted caudally through the incision (Fig. 2). The end of the breathing catheter that was external to the animal was angled so that it was clear of obstructions, thereby allowing the animal to spontaneously breathe room air. A second catheter, made from an infant feeding tube (Size 8 French, Cutter Laboratories, Berkeley, CA), was inserted through the same incision in the direction of the larynx. The function of this catheter was to conduct aerosol from the outlet of the nasal airways to the experimental apparatus for measurement during inspiration experiments, and to deliver aerosol to the nasal passages during expiration experiments. Great care was taken to place the aerosol-conducting catheter such that its introduction to the airway caused no flow obstructions; increased pressure drop as a result of flow obstructions unrelated to normal anatomy would compromise the accuracy of the deposition measurements.

After the catheters were inserted, a mask, which was constructed from latex (Dental Dam, Hygenic Corporation, Malaysia) and a funnel using silicone sealant, were positioned over the animal's external nares. Petroleum jelly was applied to the animal and latex mask to minimize air leakage. The mask and the end of the aerosol-conducting catheter that was external to the animal were then connected to the experimental flow apparatus.

To ensure proper placement of the aerosol-conducting catheter, air was passed through the nasal airways and the rise of a soap bubble in a bubble flow meter connected in series with the animal was observed. The position of the catheter was delicately manipulated to yield the highest flow rate as indicated by the flow meter. If the flow rate achieved was within a few percentage points of the unobstructed flow rate, flow through the nasal passages was considered to be unobstructed. The flow meter was then placed upstream and downstream of the animal in series with the animal, and the flow rates of air traveling through the nasal passages were measured. The positions of the catheter and mask were adjusted until the flow rates were nearly identical upstream and downstream of the animal, to insure no or minimal air leakage. The catheter

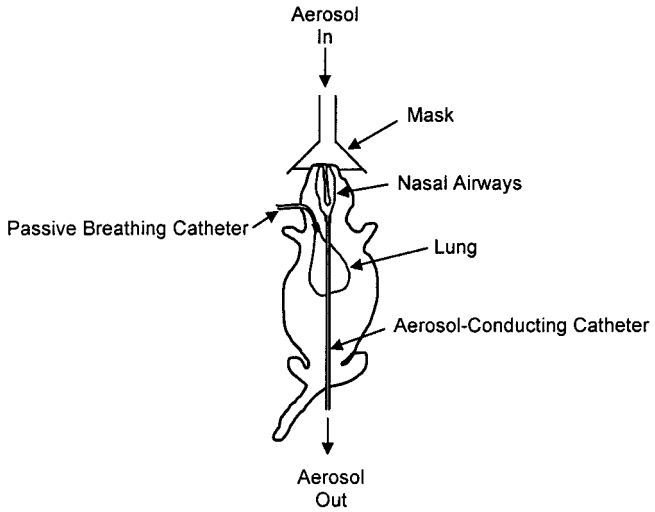


**FIG. 2.** Schematic diagram of catheter positions following surgical insertion into airway.

**TABLE 1**
**Number of Animals per Flow Condition for Surgical Methods That Included and Bypassed the Larynx**

| Flow scenario | Bypassing larynx | Including larynx | Total |
|---|---|---|---|
| Steady-state, inspiration | 6 | 4 | 10 |
| Steady-state, expiration | 5 | 1 | 6 |
| Pulsatile, inspiration | 5 | 0 | 5 |
| Pulsatile, expiration | 6 | 0 | 6 |

was secured in the optimal position with surgical thread, and petroleum jelly was applied to the incision area to eliminate air leakage from the catheter and airway interface.

The surgical procedure described above was used effectively for 5 experiments. However, because of difficulty in consistently achieving an unobstructed flow path using the surgical procedure as described, the procedure was modified for subsequent experiments. The primary cause of flow obstruction was the larynx. Various steps were taken to eliminate flow blockage by the larynx, including varying the position of the animal's head, body, and tongue; manipulating the placement of the catheter; reducing the flow rates; and gavaging the rat. None of these manipulations proved to be a consistent solution. Consequently, in subsequent experiments, the catheter was inserted anterior (instead of posterior) to the larynx, in the nasopharyngeal meatus. In this configuration, aerosol flow from the nasal passages bypassed the larynx, thereby eliminating larynx-related flow obstructions. This modification required the application of ophthalmic solution (Proparacaine Hydrochloride Opthalmic Solution USP, 0.5%; Bausch & Lomb, Tampa, FL) to the sensitive tissue surrounding the incision.

***Deposition measurements.*** Deposition measurements were recorded using the experimental apparatus employed by Kelly *et al.* (2001) with a live rat in place of the previously used nasal mold. A brief description follows.

The flow from the nebulizer was split into 2 branches: an exposure line and a bypass line (Fig. 1A). The exposure line included the animal, and the bypass line contained a constriction that equalized the pressure drops between the 2 branches. Since the branches otherwise consisted of identical components, the line losses in the 2 branches were equal. By reversing the configuration of the two 3-way valves located at the ends of the 2 branches, the flow from the exposure line was directed to a particle-detection line, while flow from the bypass line was discarded through a vacuum line and vice-versa. The particle detection line used an APS to measure particle size and concentration from the exposure and bypass lines. A mass flow controller (MKS Instruments, Model 246B, Andover, MA) and a diluter (In-Tox Products, Albuquerque, NM) were used to maintain the flow rate required by the APS. The vacuum line was used to discard flow from one of the branches while maintaining balanced flow conditions between the 2 branches; it included a filter, vacuum pump (Model 4144, Emerson, St Louis, MO), and pressure gauge (Magnehelic, Dwyer Instruments, Inc., Michigan City, IN).

The pulsatile apparatus (Fig. 1B) was assembled by inserting a rodent ventilator (Model 683, Harvard Apparatus, South Natick, MA) into the steady-state apparatus (Fig. 1A) downstream of the $^{85}$Kr neutralizer. Two passive air lines were also added to the apparatus to convert pulsed flows to steady flows upstream of the APS and vacuum pump.

To simulate inspiration, the animal was oriented in the system so that aerosols passed from the exposure mask through the nasal airways and into the catheter. The orientation of the animal was reversed to simulate expiration.

The number of animals used for the surgical and flow conditions studied are listed in Table 1. At least five animals were exposed per flow condition to account for possible intersubject variability. Typically, one animal was exposed to multiple particle sizes at one or more flow rates for a given flow condition (i.e., steady state or pulsatile) for either inspiration or expiration. A total of 27 exposures were performed using 22 animals. For 5 of the 16 steady-state cases, both inspiration and expiration were studied with the same animal. Since the animal's position could not be rotated without altering the catheter placement, an extra length of tubing was added to the exposure line to reverse the flow direction without moving the animal. The influence of this extra length of tubing on deposition was expected to be minimal for all except the largest particle sizes, where deposition may have been artificially increased due to gravitational sedimentation of particles in the exposure line.

Three measurements of particle concentration from the exposure and bypass lines were sequentially recorded by alternating the configuration of the 3-way valves (Figs. 1A and 1B). Flow rates ranged from 390 to 640 ml/min for the steady-state cases, and average flow rates ranged from 220 to 330 ml/min for the pulsatile cases. Flow rates were chosen because they corresponded to minute volumes in the physiologic range of rats, yielded the entire range of impaction-related deposition efficiencies, and were conducive to *in vivo* experiments. A bubble flow meter and stopwatch were used to measure flow rates. Average flow rates were measured for the pulsatile cases for flows pulsed with a frequency of approximately 100 strokes/min. Sample times of 30 s per aerosol concentration measurement were used for cases of steady-state flow; sample times of 45 or 60 s were used for pulsatile cases. These sample times were long enough that particle counts were well above background levels and short enough that the nebulizer output concentration remained constant during sequential measurements.

Particle concentration measurements taken from the bypass line reflected exposure concentrations at the external nares of the rat, while those taken from the exposure line represented conditions at the outlet of the nasal airways. Nasal deposition efficiency ($\eta$) was determined as follows (Gerde *et al*., 1991):

$$\eta = 1 - \frac{C_{exposure}}{C_{bypass}} \tag{1}$$

where $C_{exposure}$ and $C_{bypass}$ are the measured concentrations from the exposure and bypass lines, respectively.

Occasionally, the flow rate changed during measurements because of disruption of the catheter placement. Changes in flow rate were detected by conducting frequent flow rate measurements, observing changes in the pressure gauge reading, and occasionally by observing large changes in particle concentration. When the flow rate was observed to change during measurements, the measurements were discarded and repeated after the flow had been reset.

Slightly negative deposition efficiencies were occasionally measured as a result of minor fluctuations in nebulizer output concentration. These measurements, which occurred infrequently for the smallest particle sizes only, were discarded because of their physical impossibility. Blockage of the nebulizer jet, in addition to settling of particles in the nebulizer cup, occasionally resulted in a reduction of nebulizer output concentration to near background levels. In these instances, measurements were discarded, the problem was resolved, and measurements were repeated.

***Data analysis.*** Deposition efficiency curves were generated from experimental measurements by fitting the following model (Zhang and Yu, 1993) to the data:

$$\eta = \left[\frac{(\rho d^2 Q)^{\alpha}}{C + (\rho d^2 Q)^{\alpha}}\right]^{\beta} \tag{2}$$

where $\alpha$ and $\beta$ are constants that were determined using KaleidaGraph 3.5 (Synergy Software, Reading, PA), which employs the Levenberg-Marquardt algorithm for constant determination, and constant $C$ was fixed at a value of $10^5$ for all cases studied. For the steady-state cases, Equation 2 was fit to combined data from surgical methods that included and bypassed the larynx, because a consistent difference in deposition between data from the 2 cases was not observed. The values of the constants for the best-fit equations and associated $r^2$ values are listed in Table 2.

**TABLE 2**
**Values for Constants in Equation 2 and Associated $r^2$ Values**

| Flow scenario | $\alpha$ | $\beta$ | $r^2$ |
|---|---|---|---|
| Steady-state, inspiration | 2.399 ± 0.04 | 0.271 ± 0.02 | 0.77 |
| Steady-state, expiration | 2.611 ± 0.06 | 0.284 ± 0.03 | 0.81 |
| Pulsatile, inspiration | 2.842 ± 0.06 | 0.296 ± 0.02 | 0.84 |
| Pulsatile, expiration | 3.286 ± 0.11 | 0.28 ± 0.03 | 0.73 |

## RESULTS

Particle deposition efficiencies in rat nasal airways for steady-state flow conditions are illustrated in Figure 3 with identifiers for data from surgical methods that included and bypassed the larynx. Deposition efficiencies for pulsatile conditions are depicted in Figure 4. The error bars indicate standard deviations based on 3 measurements. Deposition efficiencies were plotted as functions of particle inertia, $\rho d^2Q$, where $\rho$ is the particle density, d is the particle geometric diameter, and Q is the volumetric flow rate. $\rho d^2Q$ is a convenient parameter for particle deposition that is physically related to inertial impaction (Heyder and Rudolf, 1977; Lippmann *et al*., 1977; Zhang and Yu, 1993). The dominant deposition mechanism for all except the smallest particles used in the study (i.e., 0.5-$\mu$m) was inertial impaction. Deposition efficiencies for a given flow scenario are expected to be equal for identical values of $\rho d^2Q$ for deposition by inertial impaction regardless of the individual values of $\rho$, d, and Q. This behavior was exhibited in Kelly *et al.* (2001): deposition efficiencies of fine and coarse aerosols in a nasal mold for various flow rate and particle size combinations formed a single, well-defined curve when plotted versus $\rho d^2Q$. In the present work, deposition efficiencies were not expected to form a curve as well defined as in the nasal-mold study because multiple animals were used, thereby introducing intersubject variability.

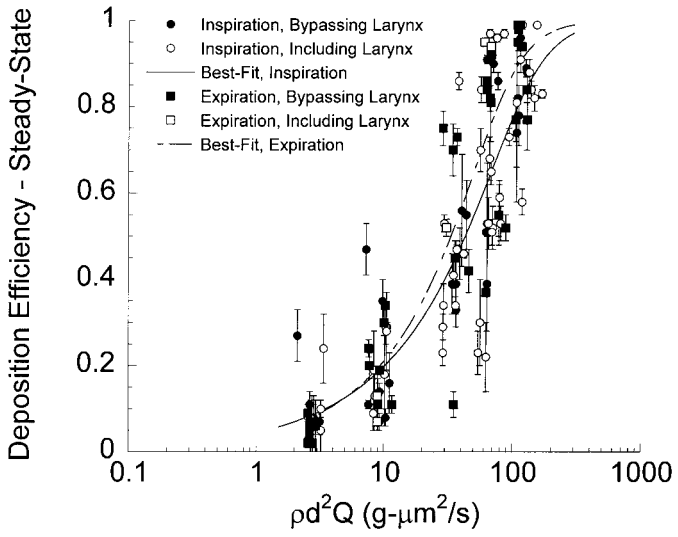


**FIG. 3.** Deposition efficiency of particles in rat nasal airways as a function of the particle inertia parameter ($\rho d^2Q$) for steady-state flow.

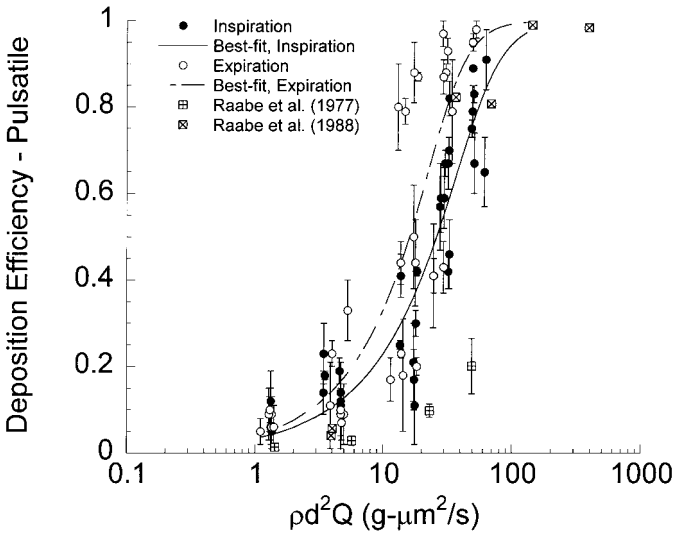


**FIG. 4.** Deposition efficiency of particles in rat nasal airways as a function of the particle inertia parameter ($\rho d^2Q$) for pulsatile flow, and experimental data from previous *in vivo* studies.

Although there was substantial variability in the data, deposition efficiency increased dramatically with increasing particle inertia for each scenario (Figs. 3 and 4). For $\rho d^2Q$ values ranging from approximately 4 to 80 g-$\mu m^2$/s, deposition efficiency increased from 0.1 to 0.7 or more for steady-state cases of inspiratory and expiratory flow (Fig. 3). For the pulsatile cases, deposition efficiency increased from approximately 0.1 to 0.7 or more as $\rho d^2Q$ values increased from 4 to 40 g-$\mu m^2$/s (Fig. 4).

The curve-fits for the steady-state cases depicted in Figure 3 indicate that the deposition efficiencies for the inspiratory and expiratory cases of steady-state flow were similar at low values of $\rho d^2Q$ (i.e., approximately 1.5–10 g-$\mu m^2$/s). For larger values of $\rho d^2Q$, expiratory deposition efficiency appeared to be somewhat higher for a given value of $\rho d^2Q$ (Fig. 3). For the pulsatile cases, expiratory deposition efficiency also appeared to be similar to inspiratory deposition efficiency for low values of $\rho d^2Q$ (i.e., approximately 1.5 g-$\mu m^2$/s) and higher than inspiratory deposition efficiency for larger values of $\rho d^2Q$ (Fig. 4).

Best-fit curves comparing deposition efficiencies for the pulsatile and steady-state cases are shown in Figure 5. At low values of particle inertia (i.e., 1.5 g/$\mu m^2$/s), the deposition efficiency for the pulsatile and steady-state cases were similar. For mid-range values of particle inertia (i.e., 15–70 g/$\mu m^2$/s), the pulsatile cases had significantly higher deposition efficiencies than the corresponding steady-state cases. At very large values of inertia (i.e., 100 g/$\mu m^2$/s), deposition efficiencies tended toward total deposition for both flow conditions.

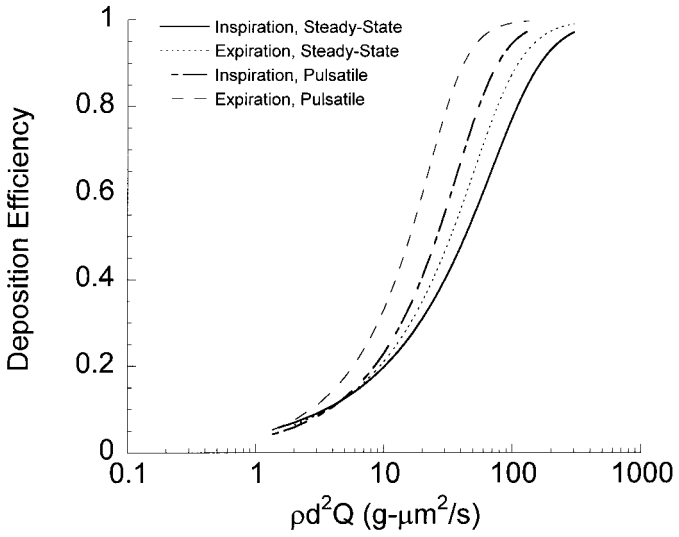


**FIG. 5.** Best-fit deposition efficiency curves of the form of equation (2) for the flow situations in the present study. Equation parameter and $r^2$ values are listed in Table 2.

## DISCUSSION

The strong dependence of deposition efficiency on the inertial impaction parameter (Figs. 3 and 4) implies that the dominant deposition mechanism for the majority of particle size and flow rate combinations was inertial impaction. For low values of $\rho d^2Q$ (i.e., 1.5 g-$\mu m^2$/s), corresponding to the smallest particle size (i.e., 0.5 $\mu$m), the deposition efficiency of the nasal airway was minimal. This result was expected because these particles do not have sufficient inertia, at the flow rates used in the study, to deviate from flow streamlines enough to cause substantial impaction; yet, these particles are large enough to prevent significant deposition as a result of Brownian diffusion. Deposition efficiencies in this size range typically represent the minimum values in deposition efficiency curves that range from ultrafine to coarse particles (e.g., Fig. 12 in Cheng *et al*., 1990). In such curves, ultrafine particle deposition increases with decreasing particle size, primarily because of Brownian diffusion, and coarse-particle deposition increases with increasing particle size and therefore inertia primarily because of inertial impaction.

Some difference in deposition between inspiratory and expiratory scenarios was expected. The flow profile in the nasal airways is different for inspiratory and expiratory flows, because the shape of the airway is asymmetrical. This difference in flow profile resulted in higher deposition for expiratory flows than inspiratory flows.

The result that particle deposition for mid-range values of particle inertia was significantly greater for pulsatile flows than steady-state flows is physically reasonable and has important implications for the study of airway deposition. For small values of particle inertia, particles closely track flow streamlines in both pulsatile and steady-state flows under conditions relevant to the study, because fluid drag forces are much larger than inertial and other forces. Therefore deposition for low values of particle inertia (i.e., 1.5 g/$\mu m^2$/s) was minimal for both flow conditions. The tracking fidelity of particles for mid-range values of particle inertia (i.e., 15–70 g/$\mu m^2$/s) is worse than for smaller values for conditions relevant to the study, because inertia hinders a particle's ability to quickly adapt its motion to fluid accelerations. Because fluid accelerations are greater in pulsatile flows than steady-state flows, particle trajectories will deviate more from flow streamlines in pulsatile flows, resulting in greater impaction deposition. Therefore particle deposition was higher in pulsatile flows than steady-state flows for mid-range values of particle inertia. For large values of particle inertia (i.e., 100 g-$\mu m^2$/s), particles do not follow flow streamlines for either flow condition, and so there was nearly total deposition in both cases. Normal breathing inherently involves fluid acceleration, and therefore, the pulsatile flow condition used in the study is probably more physiologically realistic than the steady-state condition. Thus fluid accelerations associated with normal breathing should be considered when determining deposition that is governed by inertial impaction.

A consistent relationship between deposition from scenarios that included the larynx in the flow domain and those that did not was not observed (Fig. 3). Previous work (Raabe *et al.*, 1977, 1988) has shown deposition in the larynx to be minimal compared with deposition in the nasal passages. Considering these findings, the influence of the larynx on total head deposition was probably masked by the variability in the data.

### *Previous* in Vivo *Studies*

Raabe *et al.* (1977, 1988) studied deposition of aerosols in live rat nasal airways under normal breathing conditions. The deposition data from the Raabe *et al.* studies (1977, 1988) are plotted with deposition efficiencies from the pulsatile cases of the present study in Figure 4. The Raabe *et al.* studies reported deposition in terms of deposition fraction, or fraction of the total number of particles in the exposure atmosphere that deposit in a given airway. Deposition is presented here in terms of deposition efficiency, or the fraction of the number of particles entering an airway that deposit. To facilitate comparison, reported deposition fractions (Raabe *et al.*, 1977, 1988) were converted to deposition efficiencies. The conversion was made by assuming that inspiratory and expiratory deposition efficiencies were equal and accounting for aerosol deposition in the lower respiratory tract.

Flow rates were calculated for the Raabe *et al.* studies (1977, 1988) to determine $\rho d^2Q$. For the Raabe *et al.* study (1977), the reported average male and female minute volumes were averaged, and the result was doubled, yielding a flow rate of 318 ml/min (i.e., flow rate = 2 $\times$ average min volume). For the Raabe *et al.* study (1988), the flow rate of 228 ml/min was calculated from average animal weight (205 g) using Guyton's formula (Guyton, 1947). Because of uncertainty regarding

individual minute volumes for corresponding deposition measurements, the calculated flow rates are not ideal representations of the actual flow rates.

Data from the Raabe *et al.* study (1988) agree well with deposition efficiencies from the pulsatile cases in the present study (Fig. 4). Although there are limited data available for comparison, deposition from the Raabe *et al.* (1988) study closely matches the data from the inspiratory case of pulsatile flow. Deposition from the Raabe *et al.* study of 1977 is somewhat lower than the data from the pulsatile cases used in the present study (Fig. 4). Making a thorough comparison between the Raabe *et al.* study (1977) and the present one is difficult because of the limited data available. Differences between previous work and the present study are probably the result of different study methods as well as inaccuracy in estimating the flow rates from previous studies.

### *Variability*

Due to morphological differences among the nasal airways of the rats studied, some difference in airflow patterns, and consequently in deposition, was expected among subjects. Intersubject variability was examined by comparing the deposition data acquired from different animals. Differences in the weights of animals were small and did not have a consistent relationship with deposition. The variability of the data depicted in Figures 3 and 4 was in excess of expected intersubject variability.

The surgical preparation was probably the primary source of variability. Placement of the catheter posterior to the larynx resulted in flow obstructions of varying degree, and placement of the catheter anterior to the larynx, while eliminating flow obstructions, proved difficult. Because of the limited area available for catheter placement anterior to the larynx and the soft nature of the tissue in this area, manipulation of the catheter position, which promised to yield a smoother, more physiologically realistic flow path was severely limited. Differences in flow as a result of differences in catheter placement and other factors such as animal breathing (which could influence the catheter if rapid or deep) occurred among animals.

### *Summary*

*In vivo* measurements of fine and coarse aerosol deposition in the nasal airways of female Long-Evans rats were conducted. Deposition increased sharply with increasing particle inertia for all exposure scenarios. Expiratory deposition efficiency appeared to be somewhat higher than inspiratory deposition efficiency for both steady-state and pulsatile flow conditions. Pulsatile flow yielded significantly higher deposition than steady-state flow. This result emphasizes the importance of considering fluid accelerations that are inherent in normal breathing when determining aerosol deposition that is dominated by inertial impaction. Variability in the data, which was suspected to result primarily from the difficult surgical procedure, was in excess of expected intersubject variability. Deposition results of the present work are timely, valuable data to be incorporated into extrapolation modeling and risk assessment activities for inhaled pollutants.

## ACKNOWLEDGMENTS

This research has been supported in part by grant (R827996–010) from U. S. Environmental Protection Agency's Science to Achieve Results (STAR) program and in part by CIIT Centers for Health Research core funding. The authors are also grateful to Dr. Jeffrey Everitt, R. Arden James, and Donald Joyner for their contributions to the surgical method and to Dr. Barbara Kuyper for editorial assistance.

## REFERENCES

Chen, B. T., Weber, R. E., Yeh, H. C., Lundgren, M. B., Snipes, M. B., and Mauderly, J. L. (1989). Deposition of cigarette smoke particle in the rat. *Fundam. Appl. Toxicol.* **13,** 429–438.

Cheng, Y. S., Hansen, G. K., Su, F. Y., Yeh, H. C., and Morgan, K. T. (1990). Deposition of ultrafine aerosols in rat nasal molds. *Toxicol. Appl. Pharmacol.* **106,** 222–233.

Gerde, P., Cheng, Y. S., and Medinsky, M. A. (1991). *In vivo* deposition of ultrafine aerosols in the nasal airways of the rat. *Fundam. Appl. Toxicol.* **16,** 330–336.

Guilmette, R. A., Wicks, J. D., and Wolff, R. K. (1989). Morphometry of human nasal airways *in vivo* using magnetic resonance imaging. *J. Aerosol Med.* **2,** 365–377.

Guyton, A. C. (1947). Measurement of the respiratory volumes of laboratory animals. *Am. J. Physiol.* **150,** 70–77.

Heyder, J., and Rudolf, G. (1977). Deposition of aerosol particles in the human nose. In *Inhaled Particles IV* (W. H. Walton, Ed.), pp. 107–126. Pergamon Press, Oxford.

Kelly, J. T., Kimbell, J. S., and Asgharian, B. (2001). Deposition of fine and coarse aerosols in a rat nasal mold. *Inhal. Toxicol.* **13,** 577–588.

Lippmann, M., Albert, R. E., and Peterson, H. T., Jr. (1977). The regional deposition of inhaled aerosols in man. In *Inhaled Particles III* (W. H. Walton, Ed.), pp. 105–122. Pergamon Press, Oxford.

Ménache, M. G., Miller, F. J., and Raabe, O. G. (1995). Particle inhalability curves for humans and small laboratory animals. *Ann. Occup. Hyg.* **39,** 317–328.

Raabe, O. G., Al-Bayati, M. A., Teague, S. V., and Rasolt, A. (1988). Regional deposition of inhaled, monodisperse, coarse and fine aerosol particles in small laboratory animals. In *Inhaled Particles VI* (J. Dogson, R. I. McCallum, M. R. Bailey, and D. R. Fischer, Eds.), pp. 53–63. Pergamon Press, Oxford.

Raabe, O. G., Yeh, H. C., Newton, G. J., Phalen, R. F., and Velasquez, D. J. (1977). Deposition of inhaled monodisperse aerosols in small rodents. In *Inhaled Particles IV* (Walton, W. H., Ed.), pp. 3–20. Pergamon Press, Oxford.

Schreider, J. P. (1983). Nasal airway anatomy and inhalation deposition in experimental animals and people. In *Nasal Tumors in Animals and Man* (G. Reznik, and S.F. Stinson, Eds.), Vol. 3, pp. 1–26. CRC Press, Boca Raton, FL.

Wolff, R. K., Kanapilly, G. M., Gray, R. H., and McClellan, R. O. (1984). Deposition and retention of inhaled aggregate $^{67}Ga_2O^3$ particles in beagle dogs, Fischer-344 rats, and CD-1 mice. *Am. Ind. Hyg. Assoc. J.* **45,** 377–381.

Yeh, H. C., Brinker, R. M., Harkema, J. R., and Muggenburg, B. A. (1997). A comparative analysis of primate nasal airways using magnetic resonance imaging and nasal casts. *J. Aerosol Med.* **10,** 319–329.

Zhang, L., and Yu, C. P. (1993). Empirical equations for nasal deposition of inhaled particles in small laboratory animals and humans. *Aerosol Sci. Technol.***19,** 51–56.